Research Article

Marked structural and functional heterogeneity in CXCR4: Separation of HIV-1 and SDF-1α responses

ANDREW J SLOANE,[1,2,3,4] VIC RASO,[5] DIMITER S DIMITROV,[6] XIAODONG XIAO,[6] SHIVASHNI DEO,[2,4,7] NICK MULJADI,[1,2,3] DAVID RESTUCCIA,[4,8] STUART TURVILLE,[1,2,3,4] CHRISTINE KEARNEY,[5] CHRISTOPHER C BRODER,[9] HANS ZOELLNER,[4,8] ANTHONY L CUNNINGHAM,[2,3,4] LINDA BENDALL[2,4,7] and GARRY W LYNCH[1,2,3,4,8]

[1]*HIV-Protein Interactions Laboratory, Centre for Virus Research,* [2]*Westmead Millennium Institute,* [3]*National Centre for HIV Virology Research of Australia,* [4]*University of Sydney,* [7]*Westmead Institute for Cancer Research,* [8]*Cellular and Molecular Pathology Research Unit, Department of Oral Pathology and Oral Medicine, Westmead Hospital Dental School, Westmead, NSW, Australia,* [5]*Boston Biomedical Research Institute and Harvard University Medical School, Watertown, Massachusetts,* [6]*Protein Interactions Laboratory, National Cancer Institute, National Institutes of Health, Fredrick and* [9]*Department of Microbiology and Immunology, Uniformed Services University of Health Sciences, Bethesda, Maryland, USA*

Summary CXCR4, the chemotactic cell receptor for SDF-1α, is essential for immune trafficking and HIV infection. CXCR4 is remarkably heterogeneous and the purpose of this study was to better identify the isoforms expressed by cells and compare their structure and function. We found that cells express either a predominant isoform or multiple isoforms. These were best resolved on SDS-PAGE using sucrose-gradient-fractionated, triton-insoluble, membrane extracts. We hypothesized that glycosyl modification may underpin some of this heterogeneity and that cell isoform(s) differences may underscore CXCR4's multiple cell functions. A comparison of wild-type (WT) and dual N-linked glycosylation site, N11A/N176A, mutant CXCR4 expressed in 3T3 and HEK-293 cells served to implicate variabilities in glycosylation and oligomerization in almost half of the isoforms. Immuno-precipitation of CXCR4 revealed monomer and dimer non-glycosylated forms of 34 kDa and 68 kDa from the N11A/N176A mutant, compared with glycosylated 40 kDa and 47 kDa and 73 kDa and 80 kDa forms from WT. The functional specificity of isoform action was also implicated because, despite CEMT4 cells expressing high levels of CXCR4 and 11 different isoforms, a single 83 kDa form was found to bind gp120 for HIV-1 IIIB infection. Furthermore, comparative studies found that in contrast to SDF-1α-responsive Nalm-6 cells that expressed similar levels of a single isoform, CEMT4 cells did not show a Ca^{++} flux or a chemotactic response to SDF-1α. Thus, CXCR4 can differ both structurally and functionally between cells, with HIV-1 infection and chemotaxis apparently mediated by different isoforms. This separation of structure and function has implications for understanding HIV-1 entry and SDF-1α responses and may indicate therapeutic possibilities.

Key words: CXCR4, glycoprotein 120, heterogeneity, SDF-1α.

Introduction

The importance of CXCR4 and stromal-derived factor (SDF-1α) interactions is evident from mouse SDF-1α and CXCR4 gene knockouts. Both are embryonically lethal as a result of disruption to haematopoietic, angiogenic and neural development, and have been reviewed in Juarez *et al*.[1] In the adult, CXCR4–SDF-1α interactions are central to haematopoiesis, immune responsiveness and angiogenesis.[2–5] CXCR4 is also implicated in a variety of pathological conditions, including inflammation and the metastasis of a variety of cancers.[1] In combination with CD4, CXCR4 also provides a receptor-binding complex for the HIV envelope glycoprotein (gp120), which facilitates HIV-1 cell fusion and viral entry by CXCR4 utilizing X4 strains of HIV-1.[6–10] SDF-1α and gp120 bind overlapping but distinct regions on CXCR4.[11,12] Cell surface CXCR4 reacts multifunctionally to SDF-1α exposure and promotes a variety of proliferative, differentiative, survival, morphological, chemotactic and adhesive cell responses.[1] This raises questions of whether CXCR4 has functionally different forms between cell types and how CXCR4–SDF-1α inter-actions might be mediated or controlled. These questions are particularly pertinent considering CXCR4's constitutive expression by most body tissues.[2,13,14]

Variability in cell surface expression alone appears too simplistic to explain the multiple cellular responses of CXCR4. Our initial observations revealed MW heterogeneity in CXCR4 between different cell types and suggested that the biology of CXCR4 was far more complex than has been

appreciated.[15,16] Other studies have also described a variety of different CXCR4 MW forms, such as the predominant 45–47 kDa isoforms found in MoltT4, Sup-T1 and transfected BS-C-1 cells[8,17,18] and 59–62 kDa and 90 kDa forms found in monocytes.[19] In this study, we show that other cells, including CEMT4, THP-1 and HEK-293, 3T3 and U-87 transfectants, as do transfected HeLa cells,[20] express multiple different MW isoforms. The considerable differences in the MW of the CXCR4 isoforms observed cannot simply be explained by either gene splicing[2] or genetic polymorphism.

There are, however, numerous post-translational modifications of CXCR4, including N-glycosylation,[21] disulfide formation,[22] tyrosine sulfation,[20,23] serine chondroitin sulfation,[20] oligomerization[19] and proteolysis,[24–26] that affect approximately 9% of extracellular residues as well as phosphorylation of intracellular CXCR4 sites.[27] We investigated whether N-glycosylation contributes to the different MW forms observed. We also carried out a comparative functional study examining cell calcium mobilization and chemotactic responses in cells that express different CXCR4 isoforms. This led us to hypothesize that CXCR4 isoform differences exist between cells and their differential expression may influence CXCR4-driven cell functions such as HIV-1 entry or responsiveness to SDF-1α.

Materials and methods

Chemicals and peptides

All chemicals used were from Sigma Chemicals (St Louis, MO, USA) unless otherwise stated. With the assistance of Dr R Liu and A Wong we synthesized and purified mimetic peptides of the N-termini of CXCR4 (X4NT)(aa 1–38), CCR5 (R5NT)(aa 1–31) and CCR3 (R3NT)(aa 1–34)[28] using standard f-moc chemistry. Peptide purity was assessed using mass spectrometry on a Voyager DE mass spectrometer (Perseptive Biosystems, Framingham, MA, USA). Additional CXCR4 peptides of aa 1–20 (X4N1) and aa 19–38 (X4N2) and scrambled composites of identical amino acids, namely X4N1-scr ([H]-SGDMTDGIYE-IESMGEYNTS-[NH2]) and X4N2-scr ([H]-AFGDECNKME-FNSYDNPKRE-[NH2]), and a control cytomegalovirus (CMV) UL87 peptide ([H]-SGEYDVLITD-GDGSEHNNPN-[NH2]) were obtained from Auspep (Parkville, Victoria, Australia).

Antibodies

The IgG$_1$ RL5C3 and RL3G5 mAb we raised to keyhole limpet haemocyanin (KLH) coupled X4NT peptide and prepared as previously described.[29] The 4G10 mAb is also a CXCR4 N-terminus-directed antibody.[21] The 12G5 (IgG$_{2a}$) mAb was obtained from the National Institutes of Health AIDS Research and Reference Program (Rockville, MD, USA) and from R & D Systems (Minneapolis, MN, USA) and the 171 (IgG$_{2a}$), 172 and 173 (IgG$_{2b}$) mAb from R & D Systems. The hybridomas used were cultured in protein-free hybridoma medium (PFHM-II) with L-glutamine (Life Technologies, Gaithersburg, MD, USA) and the mAb purified using 1 mL HiTrap protein G selpahose columns (Amersham Pharmacia Biotech, Uppsala, Sweden) and low-pressure chromatography procedures. Rabbit polyclonal antibody (pAb) to X4NT peptide was prepared by BioQuest (North Ryde, NSW, Australia). Additional CXCR4 pAb were obtained from Santa-Cruz Biotechnology (Santa Cruz, CA, USA) and Biochain (Hayward, CA, USA).

Primary and cultured cells

The CEMT4 and HeLa human cell lines and U87.CD4 and U87.CD4.CXCR4 glioma cell-line transfectants were obtained from the National Institutes of Health AIDS Research and Reference Reagent Program. Jurkat PM-1, THP-1, K562, MDA-MB-231, T-47D ductal and HEK-293 cell lines were obtained from the American Type Culture Collection (Rockville, MD, USA). The 3T3-CD4 cells were a gift from Dr Dan Littman (Skirball Institute of Biomolecular Medicine and Howard Hughes Medical Institute, New York University School of Medicine, NY, USA). The Nalm-6 cells were provided by Dr Ken Bradstock (Westmead Hospital, NSW, Australia). Cells were cultured in RPMI-1640 (Life Technologies) and supplemented with 10% heat-inactivated fetal bovine serum (CSL, Parkville, Victoria, Australia). The MDA-MB-231 and T-47D breast cancer cell lines were supplemented with 0.25 IU/mL human neutral insulin, Actrapid (Novo Nordisk Pharmaceuticals, North Rocks, NSW, Australia). Human umbilical vein endothelial cells (HUVEC), gingival fibroblasts, PBMC and PBL were prepared as previously described.[30–32]

Flow cytometry

Cells (1×10^6) were incubated with 1 μg of mAb at 4°C for 20 min in 10% FCS in PBS. Cells were washed in buffer (PBS, 0.1% BSA, 0.1% sodium azide, pH 7.5) by 150 g centrifugation for 5 min followed by incubation with sheep antimouse Ig-FITC conjugated secondary antibody (Becton Dickinson, San Jose, CA, USA) at 4°C for 20 min. After washing, the cells were analysed using the Cell Quest software with a FACS calibur flow cytometer (Becton Dickinson).

Preparation of cell membranes

Cells were washed twice with 0.1% BSA in PBS, pH 7.5, and resuspended to 5×10^7 cells/mL in membrane extraction buffer (0.25 mol/L sucrose together with 10 mmol/L iodoacetamide [IAA], 10 mmol/L EDTA, 1 mg/mL BSA with protease inhibitors) at 4°C.[32,33] Plasma membranes were disrupted by sonication using a Branson Sonifer 450 (Branson Ultrasonics Corporation, Danburg, CT, USA) at 30 W for two 10 s pulses at 4°C. Granule and particulate material was removed by centrifugation at 1000 g for 10 min at 4°C and membranes pelleted by ultracentrifugation at 105 000 g for 60 min at 4°C in a TL-100 ultracentrifuge (Beckman, Palo Alto, CA, USA). Pellets were resuspended in either 250 μL of non-reducing SDS-PAGE sample buffer or 200 μL of lysis buffer.[32,33] Some experiments were carried out using an alternate lysis buffer of 1% Brij-97 (polyoxyethylene 10 oleyl ether) with 30 min incubation at room temperature (RT). Lysates were subsequently centrifuged at 12 000 g for 10 min at RT to obtain the non-ionic detergent soluble and insoluble factions and processed for electrophoresis either with or without sucrose-gradient prefractionation as described previously.[34]

Immunoprecipitation, immunoblotting and biotinylation

Protein immunoprecipitation from non-ionic detergent soluble supernatant was carried out using 1 h treatment with antibodies at 4°C or with matched 1 μg/mL isotype or polyclonal control Ig.[32] Cell surface CXCR4 biotinylation, blotting and detection was carried out on cells washed in PBS and labelled using incubation with 0.25 mmol/L biotinylation reagent (biotinamidocaproate N-hydroxy succinamide ester) at RT for 30 min and processed as previously described.[32,33]

For immunoblotting, immunoprecipitates were electrophoresed on precast 4–15% acrylamide gels from Bio-Rad (Hercules, CA, USA), 4–12% polyacrylamide gels from Novex (San Diego, CA, USA) or 4–20% polyacrylamide gels from Gradipore (Frenchs Forest, NSW,

Australia) and electrotransferred to 0.2 μm nitrocellulose (Schleicher and Schuell, Keene, NH, USA).[35] After blocking, the nitrocellulose sheets were incubated at RT for 1 h with rabbit anti-CD4 (1/10 000), rabbit anti-CXCR4 (1/1000) or anti-CXCR4 primary mAb at 1 μg/mL and processed according to earlier descriptions.[32]

HIV-1 glycoprotein 120 binding studies

Biotinylation of purified IIIB HIV-1 gp120 protein (National Institutes of Health AIDS Research and Reference Reagent Program) was carried out using the EZ-Link™ NHS-LC-Biotin reagents as per the manufacturer's recommendation (Pierce, Rockford, IL, USA). Biotinylation of gp120 did not disrupt binding to CD4 as determined by soluble recombinant CD4 ELISA capture assay (data not shown). Far Western blotting was carried out using the immunoblotting method except that the antibodies were substituted with biotin-labelled gp120. To prevent the gp120 from binding to immobilized cell CD4, and to expose co-receptor binding sites, 2 μL of a 0.74 mg/mL stock of IIIB gp120 was first pre-incubated with 1.2 μL of a 5 mg/mL stock of recombinant CD4 (rCD4) for 30 min at 37°C with mixing. After SDS-PAGE and electrotransfer of protein to nitrocellulose, far Western blotting was carried out with 1.5 μg labelled gp120 in 10 mL of BSA blocking buffer for 1 h at RT. The blots were then processed as described above for biotin reactivity by the addition of a 1/2500 dilution of streptavidin-horseradish peroxidase (HRP), followed by chemiluminescence detection. Similar to the method for gp120 binding to intact cells, 2×10^6 cells/mL were incubated with unlabelled IIIB gp120–CD4 complex at 1.5 μg gp120/10^7 cells for 30 min at 37°C prior to cell washing, lysis, SDS-PAGE and nitrocellulose blotting. HIV gp120 protein was then detected by immunoblotting using a pool of anti-gp120 mAb, B13 and C12, followed by sheep antimouse-HRP conjugate detection.

Mutagenesis and recombinant vaccinia viruses

CXCR4 mutations were prepared using a QuickChange site-directed mutagenesis kit (Stratagene, La Jolla, CA, USA) in accordance with the manufacturer's instructions.[21] Two mutagenic polyacrylamide gel electrophoresis-purified oligonucleotides were used per mutation and the identities of the mutant confirmed by DNA sequencing. Recombinant vaccinia viruses encoding either wild-type (vHC-3) or dual glycosylation site N11A, N176A mutant (vHC-7), were prepared by subcloning the appropriate cDNA into the *Sma*I site of pMC1107 as previously described.[21] Purified vaccinia virus was used at a multiplicity of infection (MOI) of 20 plaque-forming units/cell for infection of cells and expression of CXCR4.

HIV-1 infection

Viral stocks of the T-tropic HIV IIIB isolate obtained from the National Institutes of Health AIDS Research and Reference Reagent Program were expanded from PHA-activated (5 μg/mL phytohaemagglutinin stimulated for 3 days) and infected PBMC (white blood cells were obtained courtesy of the Australian Red Cross Blood Transfusion Service). The virus was added to 1.5×10^5 CEMT4 cells or 1.5×10^6 PBMC cells at a MOI of 0.01. Infections were carried out for 2 h at 37°C with mixing. The cells were then washed three times and resuspended in RPMI-1640 with 10% FCS and recombinant human IL-2 (Roche Diagnostics, Alameda, CA, USA) and incubated in 24-well culture plates at 37°C. Supernatants were sampled for assay at days 4, 7, 10 and 14 post-infection, with 500 μL removed from each well after 4 and 7 days of culture and replaced with 500 μL of fresh media. Levels of infection were determined by measuring p24 Ag using a Coulter HIV-1 p24 antigen assay kit (Miami, FL, USA). Cultured cells were also visualized using phase-contrast light microscopy.

SDF-1α cell chemotaxis, calcium flux and cell binding assays

Cell chemotaxis was determined as previously described using 5 μm pore membranes for CEMT4 and 8 μm for Nalm-6 or Jurkat cells and 100 ng/mL SDF-1α as the chemoattractant.[36,37] Calcium flux assays were carried out on 10^6 cells loaded with fura-red dye (Molecular Probes, Eugene, OR, USA). The fluorescence emission ratio was followed kinetically by flow cytometry (Becton Dickinson) at 40 s of mock and 200 ng/mL SDF-1α or 2.5 μg/mL ionomyocin treatments, with the fluorescence monitored for a further 80 s. The binding of SDF-1α to cells (i.e. Nalm-6, CEMT4, Jurkat) was carried out by 30 min treatment of 10^6 cells/mL with 0.5 nmol/L to 0.5 μmol/L SDF-1α at 4°C. Cells were then treated with anti-CXCR4 phycoerythrin (PE)-conjugated mAb 12G5 at 1 μg/10^6 cells followed by flow cytometry. The SDF-1α binding was scored using the loss of mAb 12G5 binding to the respective cells.

Results

Specificity of antibodies generated against N-terminus CXCR4 peptide

Monoclonal antibodies RL5C3 and RL3G5 and a pAb to CXCR4 N-terminus peptide were shown to be specific at 0.2 μg/mL by dot blotting for CXCR4 N-terminus peptides (X4NT and X4N1 or X4N2) spotted onto nitrocellulose (1 μg to 1 ρg) (Fig. 1A,B). No cross-reactivity to scrambled peptides of CXCR4 N-terminus, CMV peptide or N-terminus peptides of CCR3 or CCR5 was detectable. As expected mAb 12G5, 171 and 173, which target different epitopes in the extracellular loops of CXCR4,[17,38,39] did not react with any of the N-terminal peptides of CXCR4, CCR3 or CCR5 (Fig. 1A). The specificity of RL5C3 and RL3G5 mAb was further confirmed using flow cytometry, with CXCR4 detected on U87.CD4.CXCR4 transfected cells but not on U87.CD4 transfected glioma cells (data not shown).

Multiple molecular weight bands detected by CXCR4 antibodies on CEMT4 cells

Initial studies on CEMT4 cell lysates for CXCR4 Ag by immunoblotting showed considerable variability in the banding patterns detected by different anti-CXCR4 antibodies, but these bands were accompanied by high backgrounds (data not shown). To enhance the clarity and resolution, the experiments were repeated and the results confirmed using cell membranes (Fig. 2). When the banding profiles of mAb RL3G5, 171, 173 and 12G5 were compared in Triton/Nonidet P-40 or Brij97 soluble fractions there were both common and different bands (Fig. 2A,B,D). The specificities of the blotting reactions were confirmed both by the lack of detection by IgG$_1$ (Fig. 2A,D) and IgG$_1$ and IgG$_{2a}$ pool (Fig. 2B) isotype control blots and more importantly by specific inhibition of anti-CXCR4 N-terminus mAb RL3G5 binding by the X4NT peptide to which this antibody was raised (Fig. 2C). Different cell lines (e.g. PM-1, THP-1) and primary cells were also examined and similar results were found (data not shown).
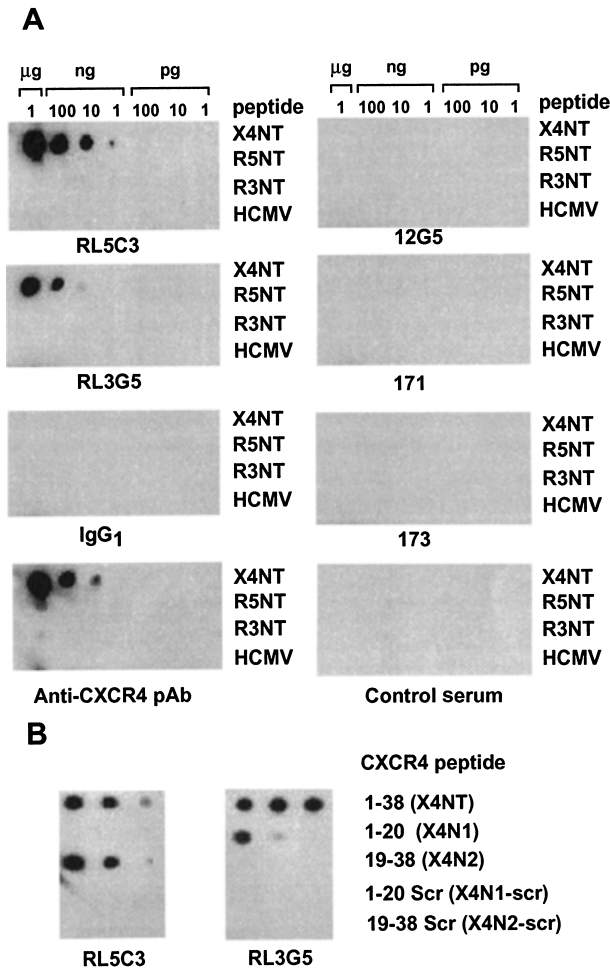
A

RL5C3 ... peptide X4NT R5NT R3NT HCMV

12G5 ... peptide X4NT R5NT R3NT HCMV

RL3G5 ... X4NT R5NT R3NT HCMV

171 ... X4NT R5NT R3NT HCMV

IgG₁ ... X4NT R5NT R3NT HCMV

173 ... X4NT R5NT R3NT HCMV

Anti-CXCR4 pAb ... X4NT R5NT R3NT HCMV

Control serum ... X4NT R5NT R3NT HCMV

B

CXCR4 peptide
1-38 (X4NT)
1-20 (X4N1)
19-38 (X4N2)
1-20 Scr (X4N1-scr)
19-38 Scr (X4N2-scr)

RL5C3 **RL3G5**

Figure 1 Immunoblotting reactivity of anti-CXCR4 antibodies to CXCR4, CCR3 and CCR5 N-terminal peptides and control peptides. The RL5C3 and RL3G5 mAb and rabbit polyclonal antibody generated to CXCR4 N-terminal peptide were examined by dot blotting for reactivity to N-terminus CXCR4, CCR3 and CCR5 peptides, sequence scrambled peptide and unrelated control cytomegalovirus (CMV) peptide. These mAb were compared with the commercial mAb 12G5, 171 and 173, and with pre-immune serum, respectively. (A) Serial dilutions of N-terminal peptides of 1 μg, 100 ng, 10 ng, 1 ng, 100 pg, 10 pg and 1 pg were spotted (1 μL) onto nitrocellulose, blocked with 'blotto' solution and incubated with 1 μg/mL of the respective mAb. Incubations were for 1 h at room temperature prior to exposure with secondary sheep antimouse horseradish peroxidase (HRP) or donkey anti-rabbit HRP conjugates, followed by chemiluminescence detection. Peptides are indicated to the right and the blotting antibody is noted beneath each blot. (B) Serial dilutions of full length N-terminus (X4NT) or peptides representing truncated N-terminus amino acids 1–20 (X4N1) and 19–38 (X4N2) or their scrambled sequence counterparts 1–20scr (X4N1-scr) and 19–38scr (X4N2-scr) were spotted and RL5C3 and RL3G5 epitope mapping carried out.

Notably, CXCR4 Ag was consistently extracted by SDS more efficiently than by non-ionic detergents (Fig. 2A,B). Multiple experiments revealed Ag with approximate MW of 40, 47, 52,

62, 70, 83 and 110 kDa as the major species repeatedly detected by mAb RL3G5 in samples extracted with Triton X-100/Nonidet P-40 and Brij-97 detergents. The 110 kDa Ag was the most prominent band observed using this mAb and using the commercial anti-CXCR4 mAb 171 and 173 (Fig. 2A,D). The migration of this band was unaffected by reduction using either 0.3 mol/L β-mercaptoethanol (Fig. 2A lane 4) or 2.5% dithiothreitol (data not shown) and this was observed for a previously described CXCR4 Ag.[19] A number of experiments also revealed high MW Ag of more than 110 kDa (Fig. 2A). In addition, mAb 171 clearly revealed a lower MW Ag form (34 kDa). For comparison the extraction efficiency of membrane CD4 was also examined in parallel (Fig. 2E) and in contrast to CXCR4 the 55 kDa monomeric CD4 was extracted with similar efficiency by all detergents (SDS recovered slightly more), but importantly without the multiple banding patterns observed with anti-CXCR4 treatments. In comparison to the multiple MW banding observed for CEMT4 and for THP-1 cells and transfected cells (Figs 3–5), we have found that there are considerable differences in the CXCR4 forms expressed by different cell types. This is evident from the expression profile for primary HUVEC cells (Fig. 2E), which when examined identically using the same mAb that reveal multiple forms in CEMT4 revealed the expression of a predominant single 110 kDa Ag in HUVEC by RL3G5 (Fig. 2E). Other examples of cells that express a single predominant isoform of CXCR4 are the 75 kDa expressing Jurkat and Nalm-6 cells (Fig. 3C). Thus, cells can be broadly grouped into two categories, those expressing a single predominant form (group A) and those expressing multiple forms (group B).

CXCR4 detection by conformational and peptide-derived anti-CXCR4 monoclonal antibodies

The immunoblotting profile of CXCR4 in CEMT4 membrane extracts detected using the peptide-raised RL3G5 mAb was compared with several commercial conformational mAbs (Fig. 2A,B,D). The 12G5 mAb poorly detected the prominent 110 kDa band shown by RL3G5, 171 and 173, but did recognize the other lower MW forms when immunoblotting was carried out at the highest sensitivity. The mAb 172 is a conformational antibody that was not reactive in immunoblotting presumably because of epitope disruption by SDS. A compilation and comparison of CXCR4 bands resolved from many experiments using a variety of anti-CXCR4 antibodies that target a range of extracellular CXCR4 epitopes is summarized in Table 1. These show considerable variability in the protein bands detected, with only three bands, measuring 34, 40 and 47 kDa and designated as isoforms α_1, α_2 and α_3, respectively, being universally detected by all antibodies.

Cell comparison for expression of the prominent 110 kDa CXCR4 isoform

The marked 110 kDa (α_{11}) isoform expressed by T-lymphoid CEMT4 cells and primary HUVEC was also compared with membrane extracts of HeLa cells, primary PBL (with and without PHA/IL-2 activation), two breast cancer cell lines (MDA-MB-272 and T-47D), a chronic myelogenous leukaemic cell (K-562) and another T cell line (PM-1) (Fig. 3A).
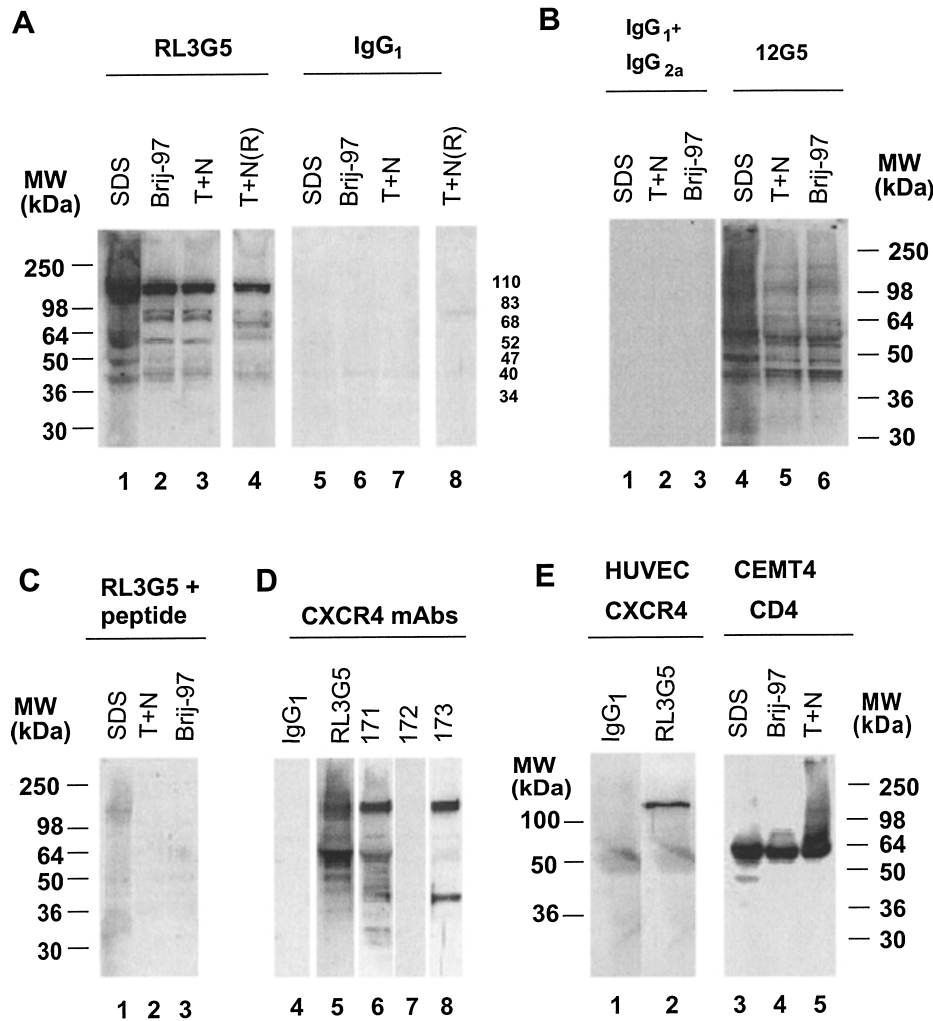
Figure 2 Detection of CXCR4 in CEMT4 and human umbilical vein endothelial cell (HUVEC) membrane extracts. CEMT4 membranes (3×10^7 cells) were prepared and proteins extracted using either 2% SDS, 1% Triton X-100, 1% Nonidet P-40 (T + N) or 1% Brij-97 and electrophoresed on 4–16% gradient SDS-PAGE followed by immunoblotting with 0.2 μg/mL of anti-CXCR4 mAb RL3G5 (A, lanes 1–4; D, lane 5), 171 (D, lane 6), 172 (D, lane 7), 173 (D, lane 8), 12G5 (B, lanes 4–6) or IgG_1 (A, lanes 5–8; D, lane 4; E, lane 1) or IgG_1 and IgG_{2a} pool (B, lanes 1–3) isotype controls (i.e. 1 μg/blot). Samples in lanes 4 and 8 were reduced with 0.3 mol/L β-mercaptoethanol prior to SDS-PAGE. (C) 0.2 μg/mL mAb RL3G5 was pre-incubated for 1 h at 37°C with 2 μg/mL of CXCR4 N-terminus peptide prior to (and during) immunoblot analysis. (D) Blotting profiles were compared for CEMT4 triton-Nonidet P-40 extracts using the different CXCR4 mAb, RL3G5, 171, 172 and 173 within the same experiment. (E) Similarly to CEMT4 cells, HUVEC were extracted using 2% SDS and immunoblotted with RL3G5. Also shown is anti-CD4 immunoblotting of CEMT4 cells revealed using a 1/10 000 dilution of the anti-CD4 pAb polyclonal T4-5 antibody (E, lanes 3–5). Blots were probed with antimouse antibody-horseradish peroxidase (HRP) conjugate (or antirabbit antibody-HRP conjugate; E right hand panel) followed by chemiluminescence detection.

This comparison demonstrated considerable variability in the expression of a single 110 kDa RL3G5 mAb detected isoform between cells, and revealed an upregulation on PBL stimulation (Fig. 3A, lanes 4 and 5). Specificity of RL3G5 binding to CEMT4 and K-562 cell extracts was demonstrated by complete blockage using pretreatment with CXCR4 N-terminus full-length (i.e. aa 1–39) X4NT and partial (aa 1–20) X4N1 peptides (Fig. 3B panels II and III) that possess the mAb binding site (defined by peptide blotting [Fig. 1] and biosensor [data not shown] epitope mapping). However, no blockage was found using epitope X4N2 (aa 19–38) peptide or control amino acid matched scrambled peptides (Fig. 3B panels IV and V).

Differences in the CXCR4 isoform profiles captured from the surfaces of CEMT4, Nalm-6 and Jurkat cells

To examine whether the multiple forms of CXCR4 are cell-surface expressed, CEMT4, Nalm-6 and Jurkat cells were cell-surface labelled by biotinylation, followed by detergent extraction and CXCR4 immunoprecipitation. The mAb 12G5 precipitated a single-surface expressed CXCR4 Ag of 75 kDa from Nalm-6 and Jurkat cells, but multiple proteins of 47–120 kDa from CEMT4 cells, which was similar to the findings from total cell membranes (Fig. 3). Immunoblotting of Nalm-6 and Jurkat cell membrane extracts also revealed a single prominent CXCR4 Ag of 75 kDa in those cells. Thus,
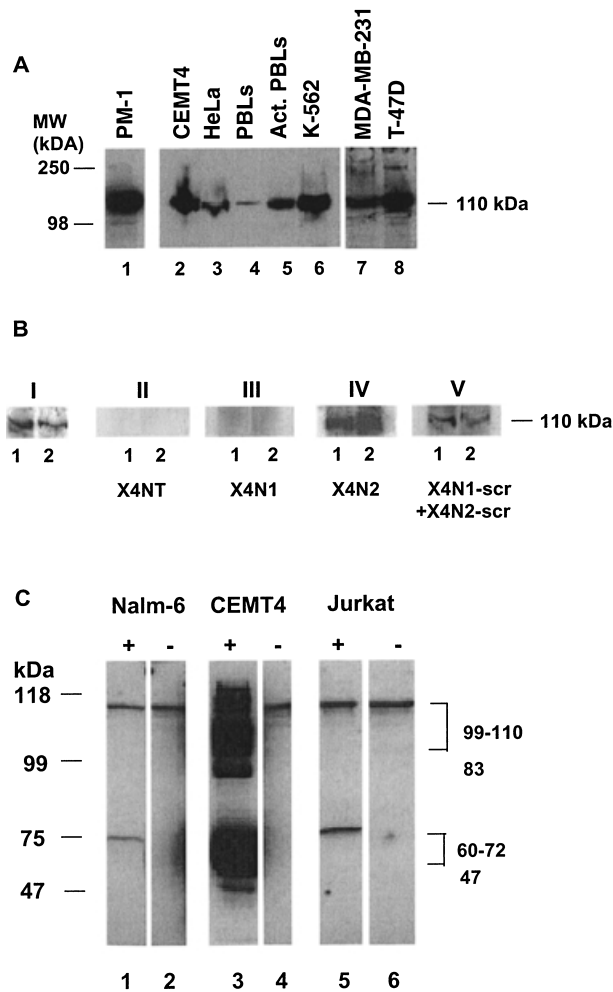
Figure 4 Examination of the CXCR4 antigen of wild-type (WT) and glycosylation site mutants. Vaccinia virus WR38 (NC) was used to express either WT or dual mutation N11A, N176A (DM) in 3T3-CD4 cells (A) or in HEK-293 cells (B). Cells were lysed in buffer containing Brij-97 and immunoprecipitation was carried out using 2 μg of mAb 4G10. The immunoprecipitation products of the DM and WT CXCR4 transfectants were compared with the vaccinia virus WR38 control (NC) alone using SDS-PAGE immunoblotting for CXCR4 (using the biochain polyclonal anti-CXCR4 antibody) (see Fig. 7A,B). In the case of (B) the X-ray film was overexposed intentionally to enhance the chemiluminescence signal to reveal the minor species. An asterisk denotes the respective CXCR4 bands.

cells variably express either a predominant CXCR4 isoform, such as the 110 kDa form of HUVEC (Fig. 2D), or the 75 kDa form of Nalm-6 and Jurkat cells (Fig. 3C), or numerous different MW forms such as the 34–110 kDa isoforms of CEMT4 cells (Figs 2,3).

Role for N-linked glycosylation in the different CXCR4 isoforms

To investigate the possibility that post-translational modification of CXCR4 could account for some of the varied SDS-PAGE mobility differences, a comparison of wild-type (WT) and CXCR4 point mutations at the asparagine glycosylation sites (Asn11 and Asn176; dual glycosylation mutant [DM]) was done. Similar to the expression of native CXCR4 in CEMT4 cells, a number of CXCR4 Ags were revealed in the WT, with mobilities of 40, 47, 62, 73 and 80 kDa (forms $\alpha_{2,4,6,7,8}$) (Fig. 4), by SDS-PAGE and immunoblotting with polyclonal anti-CXCR4. The CXCR4 Ag detected in the N11A/N176A DM mutant had fewer bands, with Ag of 34 and 68 kDa detected. Importantly, parallel treatment of the non-transfected controls was consistently negative for these bands. Thus, we concluded that non-glycosylated CXCR4 runs as a 34 kDa Ag, but that the corresponding glycosylated WT CXCR4 monomer species migrates with dual higher MW of 40 and 47 kDa. These findings also suggested that the 68 kDa species in the N11A/N176A DM immunoprecipitates represents a dimer of non-glycosylated 34 kDa CXCR4. In comparison the two bands measuring 73 and 80 kDa in WT preparations may similarly represent dimers of glycosylated CXCR4, and in the case of the 73 kDa isoform possibly a mixed heterodimer of glycosylated and non-glycosylated CXCR4. Overexposure of the WT immunoblotting profile (Fig. 4B) revealed a slight banding of 34 kDa, indicating that

Figure 3 Comparison and specificity of CXCR4 forms in membranes and on the surface of different cell types. (A) Comparison between cells types for expression of the 110 kDa CXCR4 antigen. PM-1, CEMT4, HeLa, PBL (±PHA/IL-2 activation), K-562, MDA-MD-231 and T-47D cell membranes were extracted with 2% SDS. Each sample (equal protein from 3×10^6 cells in 15 μL) was analysed by SDS-PAGE using a 4–16% polyacrylamide gradient gel followed by immunoblotting with 0.2 μg/mL of anti-CXCR4 mAb RL3G5. (B) Peptide inhibition of anti-CXCR4 mAb binding to the 110 kDa form. Membranes were prepared from CEMT4 and K-562 cells (3×10^6) (lanes 1,2) and proteins extracted using 2% SDS and analysed by SDS-PAGE. Immunoblotting using 0.2 μg/mL of anti-CXCR4 mAb RL3G5 was carried out with or without mAb pretreatment with 2 μg/mL of the following peptides for 1 h at 37°C: (I) untreated; (II) complete CXCX4 N-terminus peptide aa 1–38 (X4NT); (III) CXCR4 N-terminus peptide aa 1–20 (X4N1); (IV) CXCR4 N-terminus peptide aa 19–38 (X4N2); and (V) a mix of scrambled X4N1-scr + X4N2-scr peptides. (C) Capture of cell-surface expressed CXCR4 isoforms: comparison of Nalm-6, CEMT4 and Jurkat cells. Nalm-6, CEMT4 and Jurkat cells (2×10^7 cells) were surface labelled with biotin. Following detergent extraction the respective CXCR4 was immunoprecipitated using 1 μg/mL of 12G5 anti-CXCR4 mAb prior to SDS-PAGE. The biotinylated proteins captured were revealed by streptavidin-horseradish peroxidase (HRP) blot detection.
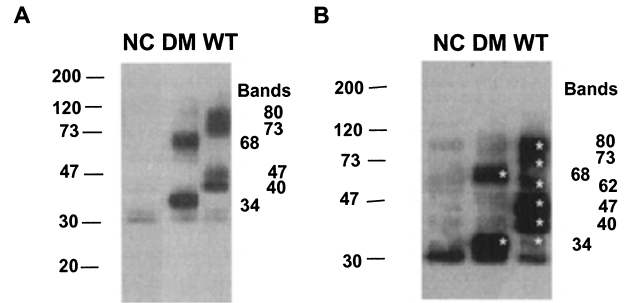
non-glycosylated CXCR4 is expressed by WT, and an additional slight band of 62 kDa. Thus, the Ag expressed in these transfected cells matched those found in CEMT4 cell membrane extracts. These results support the conclusion that variability in glycosylation and oligomerization is responsible for approximately half of the overall heterogeneity observed.

Fractionation and immunoblotting of triton-insoluble CEMT4 cell extracts

Non-ionic detergents only partially extract CXCR4 Ag from membranes (Fig. 2). Because the majority of CXCR4 partitions to a protein-rich insoluble fraction, sucrose-gradient fractionation of this component was used to further enhance protein separation. Analysis of the resulting fractions provided the best resolution of the respective isoforms by non-reduced SDS-PAGE and immunoblotting to clearly reveal CXCR4 Ag of 40, 42, 47, 52, 70 and 83 kDa by RL5C3 mAb, and additional Ag of 34, 100 and 110 (and very high MW Ag) by 171 mAb (Fig. 5B,D). Interestingly, reductive stripping of the nitrocellulose blot using β-mercaptoethanol prior to RL5C3 reprobing resulted in increased detection of the 40 and 52 kDa Ag (i.e. Fig. 5 red vs non-red), implicating epitope exposure using this procedure. Control blots of these fractions using anti-CD4 resolve the characteristic 55 kDa CD4 Ag in the absence of any non-specific or multiple other bands (Fig. 5D). Thus, sucrose-gradient fractionation of triton-insoluble extracts best resolves CXCR4 Ag (34–83 kDa). Additional blots using RL3G5 and 4G10 mAb gave comparable banding (data not shown), but RL3G5 discriminates the 110 kDa isoform. Parallel fractionation and analysis of monocytoid THP-1 cells similarly revealed multiple CXCR4 bands by RL5C3 (i.e. Fig. 5E). Sucrose-gradient fractionation as routinely used in the laboratory for separation of lipid-raft associating proteins,[34] which separate to fractions 5–8 (Fig. 5D), revealed that the CXCR4 of unstimulated CEMT4 and THP-1 cells partitions to a different, sucrose-heavy, lipid-poor, non-raft set of fractions (>9). Specificity of the multiple CXCR4 banding of CEMT4, THP-1 and transfectant 3T3 and HEK cells (Fig. 4) was further demonstrated using sucrose extracts of U87.CD4.CXCR4 compared to U87.CD4 cell fractions with multiple Ag of 62, 75 and 83 kDa in the former (Fig. 7B).

It is important to note that the multiple CXCR4 banding of the above cells contrasts markedly with other cells that express a single or predominant isoform. For example, those found in immunoblotting and surface capture experiments of HUVEC (prominent 110 kDa isoform), Nalm-6 (75 kDa Ag) (Figs 2,3) and for primary gingival fibroblasts (90 kDa) (Fig. 7A).

Figure 5 Sucrose gradient fractionation of non-ionic detergent insoluble CXCR4 from CEMT4 and THP-1 cells. The triton-insoluble pellets from 1×10^9 CEMT4 cell membranes were prepared and subjected to 5–40% sucrose gradient centrifugation. Thirteen 1 mL fractions from the top to the bottom of the gradient were collected, proteins concentrated, electrophoresed and immunoblotted using RL5C3 mAb (A). The blot was stripped under reducing conditions and re-probed with RL5C3 (B), 171 (C) and anti-CD4 antibodies (D). Similarly to the CEMT4 cells, THP-1 cell membranes were prepared, fractionated and blotted using the anti-CXCR4 mAb 5C3 (E). Fractions 4–8 correspond to classic lipid-raft-associating fractions, to which raft-associating proteins CD4 and Lck (data not shown) fractionate.

Evidence for a direct and constitutive interaction between CD4 and CXCR4

CD4 and CXCR4 have previously been co-captured along with gp120 in a tri-molecular complex.[18,40] The CXCR4 captured in those studies was the 47 kDa form from non-ionic detergent cell extracts. We examined whether native cellular CD4 and CXCR4 complexes could occur in the absence of gp120 in triton-soluble extracts. CD4 was captured by anti-CD4 (Q425) mAb immunoaffinity chromatography from CEMT4 cell lysates. Selective co-capture of the 47 kDa
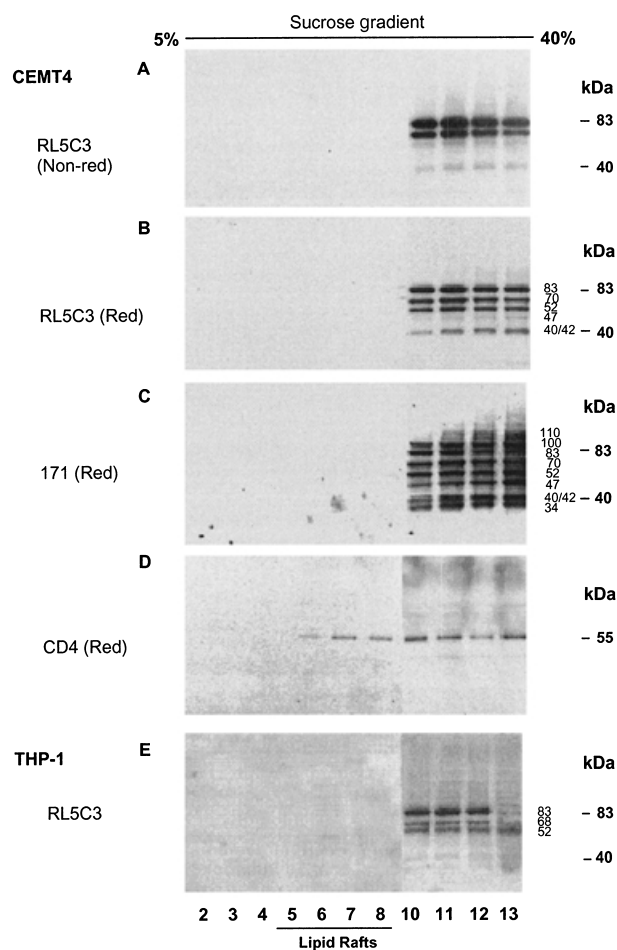
CXCR4 antigen was revealed using RL5C3 mAb immunoblotting (Fig. 6B). To examine the effect of glycosylation on the CD4–CXCR4 association, 4G10 mAb immunoprecipitations were also carried out using the glycosylation site N11A/N176A dual mutant of CXCR4 and compared with WT CXCR4 expressed in 3T3-CD4 cells. CD4 was co-captured with CXCR4 in both cases (Fig. 6C), but enhanced capture of CD4 was found in the N11A/N176A transfected cells compared with WT CXCR4, suggesting a preferential binding of CD4 to non-glycosylated CXCR4 under these conditions.

Table 1 Summary of the different non-reduced CXCR4 antigens routinely detected by immunoblotting analysis of CEMT4 cell membrane extracts using various purified anti-CXCR4 antibodies

Isoform α	MW	Anti-CXCR4 antibodies (purified)								
		RL3G5	171	173	RL5C3	4G10	12G5	Bio-chain pAb	SantaCruz pAb pool	Reference no.
11	110	+++	++	+++	–	–	–	–	–	47
10	101		+			+				47,63
9	90–95	+	++	–	–		–	++	+	19–21,47
8	80–83	++	+	–	+	++++	–	–	+	47,50
7	68–75	++	++	–	+	+	–	++	–	20,47,50,51
6	62	+	++	–	++	++++	–	–	+	19,20,47
5	52	++	+	–	±		+	–	–	24,55
4	47	++	+	+	+	+	+	++	++	8,17,19,40,44,45,47,55
3	42	+	–	±	–		+	±	–	
2	40	++	+	+	+	+	+	+	+	20,46,47
1	34	+	++	±	±	+	++	+	+	46,47

This table represents a compilation of the data from more than 100 blotting experiments. Multiple replicate experiments of immunoblotting profiles for the different anti-CXCR4 antibodies are shown. These are compared for the respective MW band forms separated by SDS-PAGE from CEMT4 cell membranes and given a relative intensity score shown by the + symbol. References from the literature are listed where evidence has been presented for CXCR4 Ag of similar MW to those observed in CEMT4 cells.
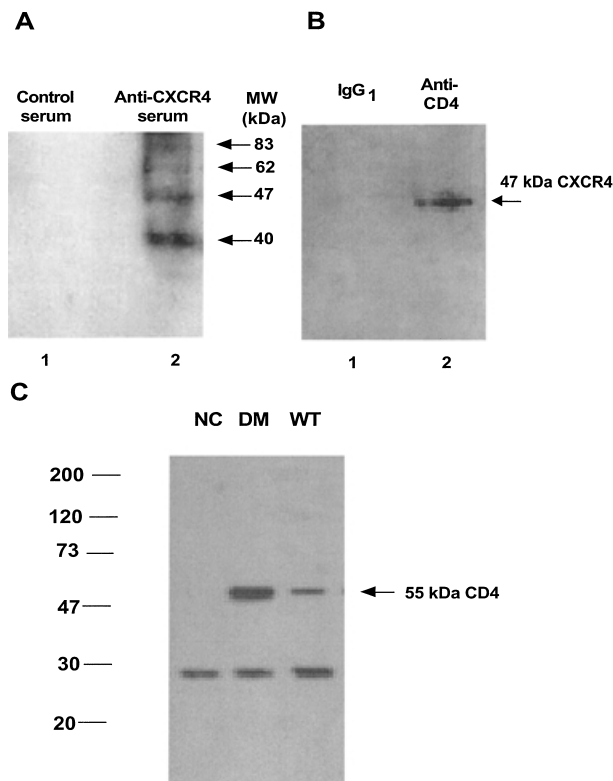
Figure 6 Extraction and detection of CXCR4 from CEMT4 cells by immunocapture and immunoblotting. (A) CXCR4 in non-ionic detergent-soluble cell extracts. CXCR4 was immuno-precipitated from 5×10^7 CEMT4 cells using either pre-immune control serum (lane 1) or an anti-CXCR4 pAb serum (BioQuest) raised against the NH2-terminus of CXCR4 (lane 2) and analysed by SDS-PAGE using an 8–16% polyacrylamide gradient gel, followed by immunoblotting with 0.2 μg/mL of the anti-CXCR4 mAb RL5C3. Note: this demonstrates that anti-CXCR4, pAb, but not pre-immune serum, captures CXCR4 Ag of 40, 42, 47, 62 and 83 kDa, further confirming the specificity of mAb immuno-precipitation, blotting and glycosylation mutant transfection studies in earlier sections. (B) Co-association of CD4 and CXCR4 in CEMT4 cells. CEMT4 cells (1×10^9) were lysed and CD4 subsequently isolated by anti-CD4 (Q425 mAb) immunoaffinity chromatography. The proteins captured were compared with proteins eluted from an IgG_1 control column prepared in parallel. An aliquot of these samples (protein from 1×10^7 cell equivalents) was analysed by SDS-PAGE followed by Western blot analysis using the anti-CXCR4 mAb RL5C3 at 1 μg/mL. (C) Co-association of CD4 with glycosylated and non-glycosylated CXCR4. The glycosylation site mutant (DM) and wild-type (WT) 3T3-CD4 transfectants, described in Figure 4, were lysed in Brij-97 lysis buffer and immunoprecipitated with anti-CXCR4 N-terminus antibody 4G10. Coprecipitation of DM and WT CD4 was determined following blotting using the anti CD4 polyclonal antibody T4-4 and compared with the vaccinia control (NC) alone.

Comparison of CXCR4 functional interactions in HIV infection and chemotaxis

Far Western blotting was carried out using biotinylated HIV-1 IIIB gp120 pre-complexed with soluble recombinant CD4 at a ratio of 4:1 to examine functional interactions. The HIV-1 gp120–rCD4 complex consistently bound strongly and selectively to the 83 kDa α_8 CXCR4 form in triton-insoluble CEMT4 extracts. Slight binding to the 40 kDa α_2 CXCR4 was also observed in some experiments (Fig. 7C). To further examine gp120–CD4 binding interactions with CXCR4, CEMT4 cells were treated with HIV gp120 in pre-complex with CD4, and the cells then lysed and extracted as for experiments used for the data in Figures 5 and 7B. The HIV-1 IIIB gp120–rCD4 that bound to intact cell CXCR4 was found to associate with the triton-insoluble membrane fraction (Fig. 7D). This was extracted as a high MW complex that migrated to the top of the SDS-PAGE gels ($\geq 1 \times 10^6$ Da). This complex when fractionated on sucrose gradients was resolved in fractions 11–13, to which CXCR4 also extracts (Fig. 5). In parallel infection studies CEMT4 cells underwent productive infection by HIV-1 IIIB with 1560 ± 40 ng/mL of p24 core HIV-1 Ag
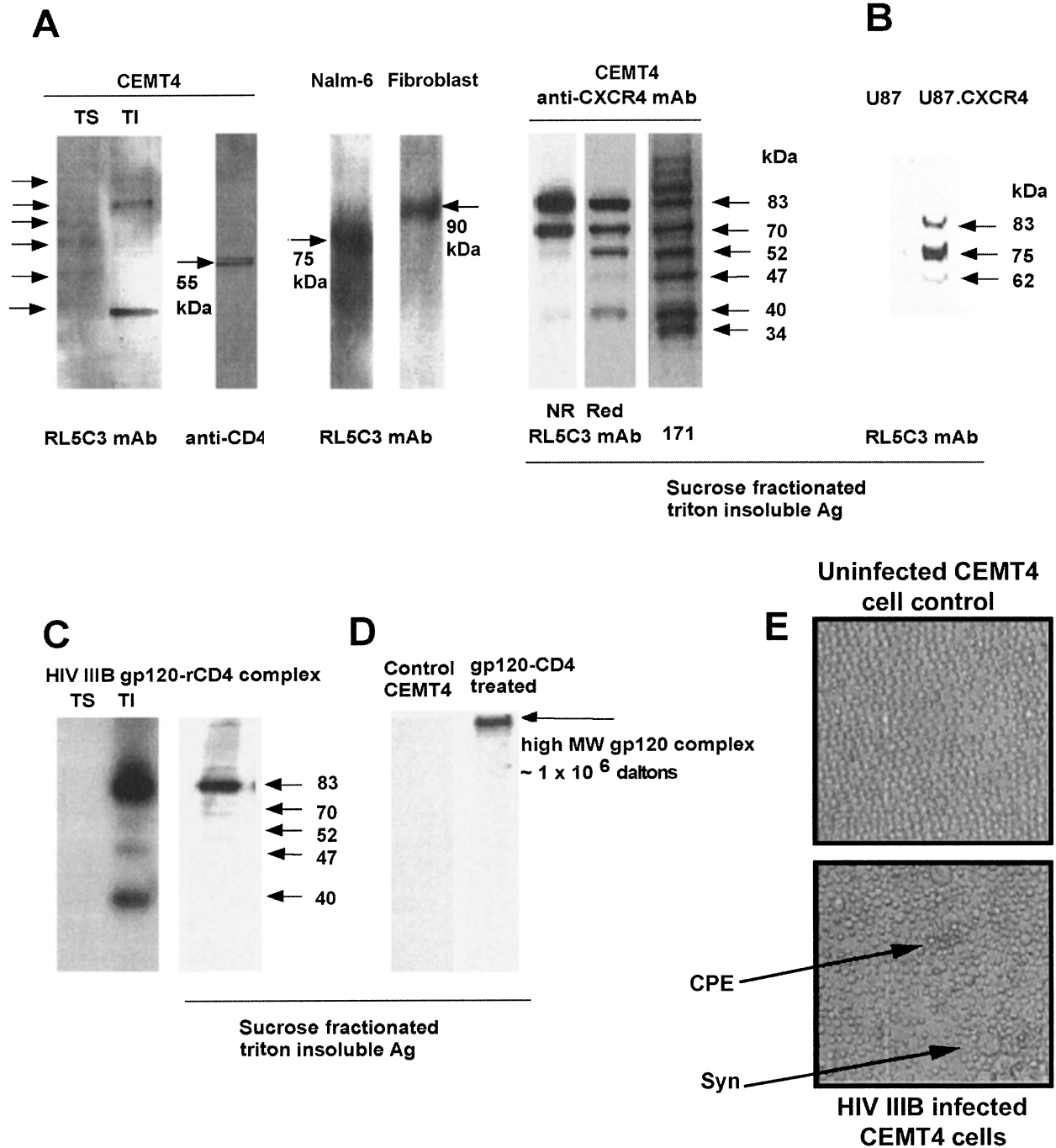
Figure 7 *Legend next page.*

detected at 7 days postinfection and this was accompanied by HIV-1-related cell cytopathic effects and syncytium formation revealed by microsopy (Fig. 7E).

Despite the capacity of CEMT4 cell CXCR4 to be functionally responsive to X4 utilizing HIV-1, CXCR4 functional responses to SDF-1α were found to be impaired. This was evident when CEMT4 cells were compared and examined in parallel with the B-lymphoid cell Nalm-6 and T-lymphoid Jurkat cells. All three cell types showed equivalent high-cell surface expression of CXCR4 (Fig. 8A). However, in contrast to Nalm-6 and Jurkat cells, where the 172 and 12G5 mAb

bind at comparable high levels, there was a considerable difference in 172 and 12G5 mAb binding to CEMT4 cells. This result suggested differences in the exposure of the mAb epitopes by CXCR4 isoforms of CEMT4 cells (with 172 markedly greater than 12G5 epitopes) compared with the more homogeneous CXCR4 protein of Nalm-6 and Jurkat cells. In functional calcium flux studies using fura-red loaded cells, Nalm-6 cells provided a strong Ca++ flux response with exposure to SDF-1α, a response that was not observed for either CEMT4 or Jurkat cells (Fig. 8B). However, each cell type did produce a strong Ca++ flux with exposure to a

Figure 7 (*from previous page*). Expression of CXCR4 in non-ionic detergent-insoluble cell extracts: preferential binding of HIV gp120 to the 83 kDa CXCR4 of CEMT4. (A) Comparison of CXCR4 banding of detergent-insoluble cell extracts. CEMT4 cells (1×10^7) were lysed and non-ionic detergent soluble (TS) and insoluble (TI) membrane extracts compared by immunoblotting using RL5C3 (left hand panel). For comparison re-blotting of the TI fraction with anti-CD4 demonstrates the single 55 kDa band of CD4. Similarly, the CXCR4 profiles obtained using RL5C3 for Nalm-6 and human gingival fibroblasts are included (A, central panels). For reference the non-ionic detergent-insoluble extracts fractionated by sucrose gradient centrifugation (Fig. 7) and immunoblotted with 171 and RL5C3 (A, right hand panels) are included. (B) Immunoblotting for CXCR4 Ag in U87.CD4 and U87.CD4.CXCR4 cell extracts. U87.CD4 and stably transfected U87.CD4.CXCR4 cells (1×10^7 cells) were treated as for the CEMT4 cell separations described in Figure 5, with sucrose fractionations performed in parallel and anti-CXCR4 mAb RL5C3 immunoblotting profiles compared. (C) Far Western blotting of HIV gp120 (IIIB) to CXCR4 extracts. Biotinylated HIV gp120 (IIIB) precomplexed with soluble recombinant CD4 at a ratio of 4:1 was incubated with blots of TS, TI and TI-sucrose fractionated CEMT4 cells to give 1.5 µg of gp120 per blot. Blots were then probed with streptavidin-horseradish peroxidase (HRP) followed by chemiluminescence detection. (D) HIV gp120–rCD4 localization to triton-insoluble cell compartment. HIV IIIB gp120-rCD4 complex was incubated at 1.5 µg gp120 with 1×10^7 CEMT4 cells in 200 µL. The cells were washed, lysed and the proteins separated by SDS-PAGE and electrotransferred to nitrocellulose. HIV IIIB gp120 was detected using a pool of anti-gp120 mAb and was found to extract in the triton-insoluble compartment with CXCR4 as shown in (C). HIV gp120 migrates non-reduced on SDS-PAGE as a high MW protein complex at the top of SDS-PAGE gels. (E) HIV IIIB infection of CEMT4 cells. CEMT4 cells (1×10^6) were infected with HIV IIIB for 2 h at a multiplicity of infection (MOI) of 0.01. HIV viral p24 assay at 7 days post-infection with mock infected controls of 0 p24 Ag and infected CEMT4 cells 1560 ± 40 ng/mL p24. HIV IIIB infected PBMC infected in parallel gave p24 readings of 98 ± 2 ng/mL with mock controls of 0 ng/mL. Microscopic examination of the HIV IIIB infected CEMT4 cells is shown in (E, bottom panel) versus uninfected controls (E, top panel). Arrows indicate the formation of syncytia (Syn) and cytopathic effects (CPE) in the HIV-1 infected panel of cells.

positive control ionomyosin stimulus. A further functional discrepancy was observed because CEMT4 cells did not show a chemotactic response to 200 ng/mL of SDF-1α (Fig. 8C). This result directly contrasted with a marked chemotactic response by Nalm-6, and to a lesser degree by Jurkat cells, following exposure to SDF-1α. Therefore, experiments were carried out to determine whether the lack of chemotactic and calcium flux CEMT4 responses resulted from a failure to bind SDF-1α. Thus, SDF-1α binding to each cell type was evaluated for its capacity to block 12G5 binding. Following pretreatment of cells with SDF-1α, concentration-dependent inhibition of 12G5 binding to all cell types was recorded (Fig. 8D). At 0.5 µmol/L of SDF-1α this resulted in 80%, 60% and 30% inhibition of 12G5 binding to the surface of Jurkat, Nalm-6 and CEMT4 cells, respectively. Although SDF-1α did not bind to CEMT4 cell CXCR4 at the same level as the other cell types, this result did indicate significant binding to CEMT4 cells and suggests a functional block downstream of binding. Thus, despite high surface expression of CXCR4, binding and infection by T-tropic HIV-1, CEMT4 cell CXCR4 neither facilitates a calcium flux nor a chemotactic response to SDF-1α.

Discussion

It is intriguing how CXCR4, a widely expressed multi-functional protein pivotal to many essential processes, can discriminately mediate different activities. In the present study we examined whether CXCR4-mediated chemotaxis and HIV-1 cell entry can occur independently. We provide compelling evidence that T-lymphoid CEMT4 CXCR4 is functional for X4 HIV binding and infection, and for binding SDF-1α, but is refractory for SDF-1α-mediated chemotaxis and calcium flux responses. Whether SDF-1α can affect other cell morphological, adhesive, proliferative, differentiative or cell survival functions remains to be determined. Our findings may be supported by earlier studies that demonstrated different intracellular signalling responses to SDF-1α and HIV-1

X4 gp120,[41] and separation of pertussis toxin sensitive[42] and insensitive[43] pathways. A full delineation of those structures, pathways or blocks that disable the respective cell responses may enable control points to be identified and targeted.

Biochemical extraction of the hydrophobic 7-transmembrane (7-TM) spanning CXCR4 from cell membranes is difficult. Brij-97 has been the main detergent used[18,44,45] and we found it to be equivalent to other non-ionic detergents (Triton X-100, Nonidet P-40). However, there was surprising variability in the immunoblotting profiles using different anti-CXCR4 antibodies, both within and between cells. CXCR4 Ag of varying MW have previously been reported,[8,19,46] resulting in some confusion. We now find that cells can be broadly grouped into two categories based on their CXCR4 SDS-PAGE expression profiles. Group A cells, such as Nalm-6 and Jurkat cells (75 kDa CXCR4), primary gingival fibroblasts (90 kDa) and primary HUVEC (110 kDa) cells, express a predominant but different species (Figs 2,3,5). Group B cells, including CEMT4, THP-1, overexpressed cell transfectants (HeLa,[20] HEK-293 cells) and primary lymphocytes,[47] express multiple isoforms (Figs 2–7). In our focused study of CEMT4 cells, a naturally derived subclone of CEM isolated from an acute lymphoblastic leukaemic individual, using 15 specific CXCR4 antibodies, we identify and classify 11 different MW isoforms (α_{1-11}) from membrane concentrates (up to 10^{10} cell equivalents) in this single cell type (Table 1).

The predominant CXCR4 Ag highlighted in the literature is the 46–47 kDa (α_4) form first described in transfected BS-C-1 cells[8] and then subsequently in MOLT4, CEM, SupT1, U937 cell lines, non-human Mink.CD4, 3T3.CD4.401 and transfected mouse BAF-B03 pro-B cells.[17,18] Additional forms of 59 kDa and 62 kDa (α_6) have also been described in primary monocytes.[19] Small MW differences could result from post-translational modification, from gene deletion or differential splicing of CXCR4 mRNA transcripts.[2] The net effect of the latter would, however, be unlikely to be discriminated by SDS-PAGE unless accompanied by additional post-translational effects.
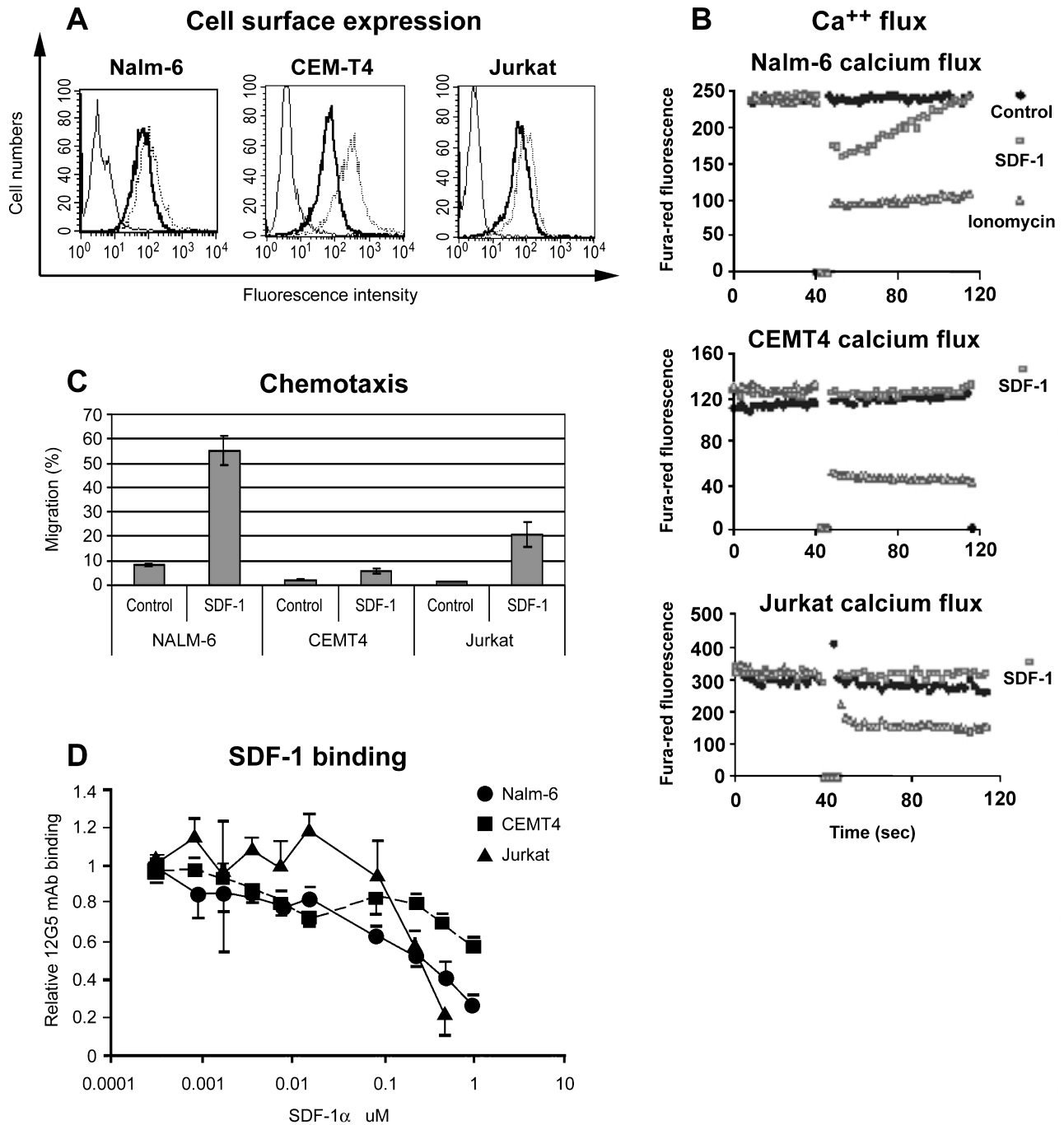
Figure 8 Comparison of cell surface expression and SDF-1α responsiveness in Nalm-6, CEMT4 and Jurkat cells. (A) Cell surface expression of CXCR4. Nalm-6, CEMT4 and Jurkat cell CXCR4 expression was determined by flow cytometry using the anti-CXCR4 12G5 (thick grey lines) or 172 (stippled) mAb and compared with matched isotype controls (solid grey). (B) The calcium flux responses of 5×10^5 Nalm-6, CEMT4 and Jurkat cells were determined by fluorescence emission ratio determinations of fura-red loaded cells followed by flow cytometry, either untreated or treated with 200 ng/mL SDF-1α or with 2.5 µg/mL ionomycin. (C) Nalm-6, CEMT4 and Jurkat cells were tested in transwell chemotaxis assay after 3 h at 37°C for chemotactic responsiveness with or without the addition of 100 ng/mL SDF-1α. (D) The binding of SDF-1α was determined by blockage of 12G5 binding to Nalm-6, CEMT4 and Jurkat cells (1×10^6 cells/mL). Cells were incubated with varying doses 0.0005–1 µmol/L of SDF-1α for 30 min at 4°C, followed by labelling with 12G5 phycoerythrin (PE) -conjugated anti-CXCR4 mAb. 12G5 binding was then analysed by FACS analysis and values scored as a relative value (0–1) compared with binding in the absence of SDF-1α.

To address whether N-glycosylation contributed to the observed heterogeneity, CXCR4 with alanine substitutions at glycosylation sites, N11 and N176 (DM), was examined.[21] Expression of the N11A/N176A DM in mouse fibroblast 3T3 and in HEK-293 cells provided a different Ag banding pattern on SDS-PAGE immunoblotting from WT CXCR4. In DM transfectants a 34 kDa Ag was found, indicating a migration of non-N-glycosylated CXCR4 on SDS-PAGE with lower apparent MW than the 39.7 kDa predicted from the primary sequence.[28,48] A similar MW Ag has also been reported for the related CCR5 monomer.[45] In comparison to DM, vaccinia infected WT gave bands of 40 kDa and 47 kDa as well as a very slight 34 kDa Ag, all of which match corresponding Ag of CXCR4 natively expressed by CEMT4 cells. Consequently, we conclude that these represent non-glycosylated (34 kDa) and differentially glycosylated (40 and 47 kDa) CXCR4. These three forms were also revealed in HEK-293 transfection and tunicamycin treatment studies.[20] Therefore, N-glycosylation is one factor in addition to splicing,[2] tyrosine sulfation and serine chondroitin sulfation[20] that contributes to the diversity of CXCR4 structures expressed by cells. The apparent 6 kDa and 13 kDa differences in MW between differentially glycosylated CXCR4 we recorded in the present study compares with earlier findings indicating that asparagine 11 glycosylation involves a 5–6 kDa carbohydrate moiety,[21] as well as an approximate 10 kDa difference between native and endoglycosidase-F-treated CXCR4.[49]

In addressing the high MW forms detected, CXCR4 can associate as tight non-covalent oligomers, can form complexes with ubiquitin, and may be induced to dimerize by SDF-1α ligation or heterodimerize with a CCR2 mutant.[19,47,50,51] As the N11A/N176A mutant CXCR4 was expressed as 34 kDa (monomer) and 68 kDa forms, the latter presumably represent homodimers of non-glycosylated CXCR4. Correspondingly, WT Ag of 73–75 kDa and 80 kDa may represent dimers of variably glycosylated CXCR4 structures. A study using MOLT4 cells also reported 40 kDa monomers and 80 kDa dimers.[46] Whether the 80–83 kDa CXCR4 are homodimers or heterodimers similar to the SDF-1α-induced heterodimers[50] remains to be determined. A high MW non-reducible CXCR4 Ag of 90 kDa in monocyte-derived macrophages (MDM) with different biochemical properties to monomeric CXCR4 has also been described.[19] Our study revealed a prominent CEMT4 Ag of 110 kDa (α_{11}), which was also the predominant CXCR4 isoform expressed by primary HUVEC. This form is also upregulated in activated PBL (Fig. 3). Furthermore, RL5C3 mAb detected the 40 kDa (α_2) and 52 kDa (α_5) forms on reduced but not unreduced blots (Fig. 5). As RL5C3 is directed to an N-terminus epitope (aa 20–38) comprising cysteine (aa 28), this may be evidence for CXCR4 with mixed open and closed disulfide configurations similar to the insulin receptor ectodomain.[52]

Glycosylation and oligomerization differences could have ramifications for CXCR4 usage by X4, R5 and dual tropic HIV because N-linked glycosylation of the N-terminus[21] can alter viral tropism and HIV infection.[21,53,54] Other CXCR4 post-translational alterations, such as cell surface N-terminus enzymatic cleavage[24–26] and tyrosine sulfation, but not serine chondroitin sulfation,[20] can also affect functional CXCR4 binding interactions with SDF-1α. Such findings support the idea that there are a variety of post-translational CXCR4 modifications that can differ between cells and modify CXCR4 functions.

Marchese and Benovic have described a 54 kDa CXCR4 in CEM cells[55] and Lapham *et al*. have described forms of 62, 75–80 and 95–100 kDa,[47] which have been found to be CXCR4–ubiquitin complexes. In this study we have assessed CXCR4 association with the primary HIV-1 receptor CD4 and have found a constitutive, but SDS-sensitive, association between the 47 kDa CXCR4 isoform (α_4) and CD4 in CEMT4 cells. CXCR4 (47 kDa, α_4)–CD4 associations have also been described in highly expressing cell transfectants,[18,19,40,44,45] which is consistent with a constitutive low affinity association. Such an association is possibly enhanced by overexpression.[44] A small core of co-localized CD4–CXCR4 membrane associations would provide a foundation for the formation of HIV Env–CD4–CXCR4 multimers to facilitate virus–cell membrane fusion.[40,44]

The extraction of CXCR4 by non-ionic detergents, as generally performed, was markedly less than the extraction by SDS because the predominant membrane CXCR4 pool in CEMT4 and THP-1 cells is triton insoluble. This may have functional relevance because HIV budding, and possibly HIV binding and fusion in lymphocytes, may involve triton-insoluble, lipid-raft membrane microdomains[9,56,57] to which signalling proteins concentrate[58–61] and CCR5 and CXCR4 may co-localize.[56,59] Prefractionation by buoyant density facilitated clear visualization of CXCR4 isoforms; however notably, CXCR4 fractionated separately from lipid-raft fractions to which characteristic raft markers, such as CD4 (Fig. 5), Lck and GM1 (data not shown), localize.

Evidence to support specific functional isoform usage was evident from the finding that of the 11 resolved CXCR4 Ag in CEMT4 cells, HIV-1 IIIB gp120–rCD4 complex bound selectively to the 83 kDa α_8 form. Further studies are required to characterize this form and to determine the exact composition and stoichiometry of the high MW gp120 SDS-resistant complex extracted from rgp120-treated CEMT4 cells that barely enters 4% SDS-PAGE gels.

A most notable result was that CEMT4 cells, despite high levels and the expression of multiple isoforms of CXCR4 and the binding and infection by T-tropic IIIB HIV-1, neither calcium flux nor respond chemotactically to SDF-1α. The latter block in CXCR4 responses appears to be post-binding because CEMT4 cells do bind SDF-1α, albeit at lower levels than Nalm-6 cells (Fig. 8D). In contrast, Nalm-6 and Jurkat cells, which express a single CXCR4 isoform of 75 kDa, do chemotax to SDF-1α (Fig. 8). However, functional differences in those cells are also apparent because Nalm-6 cells on exposure to SDF-1α undergo a calcium flux, but Jurkat cells do not. Other researchers have also found that some high CXCR4-expressing primary pre-B acute lymphocytic leukaemic cells undergo calcium flux, but not chemotaxis to SDF-1α.[37] The 75 kDa isoform implicated in the chemotactically responsive Nalm-6 and Jurkat cells appears to be very low in or even absent from CEMT4 cells and may explain their SDF-1α unresponsiveness. More definitive delineation of the CXCR4 Ag of CEMT4 cells, Nalm-6 and HUVEC, particularly of the respective 83, 75 and 110 kDa isoforms, is needed.

These studies show for the first time that the important CXCR4 functions of chemotaxis and HIV infection can occur

independently. This may permit them to be separately targeted therapeutically. In summary we have shown that: (i) CXCR4 is highly heterogeneous with different MW forms expressed by cells; (ii) some cells coexpress multiple MW isoforms; (iii) these isoforms arise in part from post-translational CXCR4 modification through N-glycosylation and oligomerization; (iv) there is constitutive association between CD4 and the 47 kDa CXCR4 form in CEMT4 cells; (v) HIV-1 IIIB gp120 binds selectively to the 83 kDa form; (vi) chemotaxis can occur both with and without an accompanied calcium flux; and (vii) there is functional separation of SDF-1α chemotaxis and HIV-1 X4 infection responses.

Our observations promote the hypothesis that cell-specific isoform expression underlies cell-specific CXCR4 functions. Whether these occur through an uncoupling of signalling or by other means,[62] a direct causal relationship remains to be demonstrated. Full characterization of each of the CXCR4 isoforms, their post-translational modifications, ligand binding and the inter-protein associations that are necessary for organogenesis, haematopoiesis, chemotaxis, immune responses, cancer and HIV infection is ultimately required.

Acknowledgements

References

1 Juarez J, Bendall L, Bradstock KF. Chemokines and their receptors as therapeutic targets: the role of the SDF-1/CXCR4 axis. *Curr. Pharm. Des.* 2004; **10**: 1245–59.

2 Gupta SK, Pillarisetti K. CXCR4-Lo: molecular cloning and functional expression of a novel human CXCR4 splice variant. *J. Immunol.* 1999; **163**: 2368–72.

3 Murphy PM. Chemokines and the molecular basis of cancer metastasis. *N. Engl. J. Med.* 2001; **345**: 833–5.

4 Rossi D, Zlotnik A. The biology of chemokines and their receptors. *Annu. Rev. Immunol.* 2000; **18**: 217–42.

5 Sallusto F, Mackay CR, Lanzavecchia A. The role of chemokine receptors in primary, effector, and memory immune responses. *Annu. Rev. Immunol.* 2000; **18**: 593–620.

6 Choe H, Farzan M, Sun Y *et al.* The beta-chemokine receptors CCR3 and CCR5 facilitate infection by primary HIV-1 isolates. *Cell* 1996; **85**: 1135–48.

7 Doranz BJ, Rucker J, Yi Y *et al.* A dual-tropic primary HIV-1 isolate that uses fusin and the beta-chemokine receptors CKR-5, CKR-3, and CKR-2b as fusion cofactors. *Cell* 1996; **85**: 1149–58.

8 Feng Y, Broder CC, Kennedy PE, Berger EA. HIV-1 entry cofactor: functional cDNA cloning of a seven-transmembrane, G protein-coupled receptor. *Science* 1996; **272**: 872–7.

9 Dimitrov DS. Cell biology of virus entry. *Cell* 2000; **101**: 697–702.

10 Dimitrov DS. Virus entry: molecular mechanisms and biomedical applications. *Nat. Rev. Microbiol.* 2004; **2**: 109–22.

11 Bleul C, Farzan M, Choe H *et al.* The lymphocyte chemoattractant SDF-1 is a ligand for LESTR/fusin and blocks HIV-1 entry. *Nature* 1996; **382**: 829–33.

12 Oberlin E, Amara A, Bachelerie F *et al.* The CXC chemokine SDF-1 is the ligand for LESTR/fusin and prevents infection by T-cell-line-adapted HIV-1. *Nature* 1996; **382**: 833–5.

13 Hazan U, Ignacio A, Cancello R *et al.* Human adipose cells express CD4, CXCR4, CCR5 and receptors: a new target cell type for the immunodeficiency virus-1? *FASEB J.* 2002; **16**: 1254–6.

14 Moore MA. The role of chemoattraction in cancer metastases. *Bioessays* 2001; **23**: 674–6.

15 Lynch G, Sloane A, Muljadi N *et al.* CXCR4 heterogeneity in expression, localisation, structure and binding to HIV gp120. *Scand. J. Immunology* 2001; **54** (Supp 1): 42 (Abstract 347).

16 Sloane A, Cunningham A, Lynch G. Studies on CD4 and the chemokine receptor HIV entry cofactors of lymphocytes and monocytes. Annual Conference of the Australian Society for HIV Medicine (IS 69). AIDSLINE National Library of Medicine: MED/98095134, 1997. Available from: http://www.aegis.com/aidsline/1994/apr/m9840034.html

17 Endres MJ, Clapham PR, Marsh M *et al.* CD4-independent infection by HIV-2 is mediated by fusin/CXCR4. *Cell* 1996; **87**: 745–56.

18 Lapham CK, Ouyang J, Chandrasekhar B, Nguyen NY, Dimitrov DS, Golding H. Evidence for cell-surface association between fusin and the CD4–gp120 complex in human cell lines. *Science* 1996; **274**: 602–5.

19 Lapham CK, Zaitseva MB, Lee S, Romanstseva T, Golding H. Fusion of monocytes and macrophages with HIV-1 correlates with biochemical properties of CXCR4 and CCR5. *Nat. Med.* 1999; **5**: 303–8.

20 Farzan M, Babcock G, Vasilieva N *et al.* The role of post-translational modifications of the CXCR4 amino terminus in stromal-derived factor 1 alpha association and HIV entry. *J. Biol. Chem.* 2002; **277**: 29 484–9.

21 Chabot DJ, Chen H, Dimitrov DS, Broder CC. N-linked glycosylation of CXCR4 masks coreceptor function for CCR5-dependent human immunodeficiency virus type 1 isolates. *J. Virol.* 2000; **74**: 4404–13.

22 Chabot D, Zhang P, Quinnan G, Broder C. Mutagenesis of CXCR4 identifies important domains for human immunodeficiency virus type 1, X4 isolate envelope-mediated membrane fusion and virus entry and reveals cryptic coreceptor activity for R5 isolates. *J. Virol.* 1999; **73**: 6598–609.

23 Farzan M, Mirzabekov T, Kolchinsky P *et al.* Tyrosine sulfation of the amino terminus of CCR5 facilitates HIV-1 entry. *Cell* 1999; **96**: 667–76.

24 Lapidot T, Petit I. Current understanding of stem cell mobilization. The roles of chemokines, proteolytic enzymes, adhesion molecules, cytokines, and stromal cells. *Exp. Hematol.* 2002; **30**: 973.

25 Levesque J, Hendy J, Takamatsu Y, Simmons P, Bendall L. Disruption of the CXCR4/CXCL12 chemotactic interaction during hematopoietic stem cell mobilization induced by GCSF or cyclophosphamide. *J. Clin. Invest.* 2003; **111**: 187–96.

26 Valenzuela-Fernandez A, Planchenault T, Baleux F *et al.* Leukocyte elastase negatively regulates Stromal cell-derived factor-1 (SDF-1)/CXCR4 binding and functions by amino-terminal processing of SDF-1 and CXCR4. *J. Biol. Chem.* 2002; **277**: 15 677–89.

27 Orsini MJ, Parent JL, Mundell SJ, Benovic JL, Marchese A. Trafficking of the HIV coreceptor CXCR4. Role of arrestins and identification of residues in the c-terminal tail that mediate receptor internalization. *J. Biol. Chem.* 1999; **274**: 31 076–86.

28 Samson M, Stordeur P, Labbe O, Soularue P, Vassart G, Parmentier M. Molecular cloning and chromosomal mapping of a novel human gene, ChemR1, expressed in T lymphocytes and polymorphonuclear cells and encoding a putative chemokine receptor. *Eur. J. Immunol.* 1996; **26**: 3021–8.

29 Yorifuji H, Anderson K, Lynch GW, Van de Water L, McDonagh J. B protein of factor XIII: differentiation between free B and complexed B. *Blood* 1988; **72**: 1645–50.

30 Chang M, Kuo M, Hahn L, Hsieh C, Lin S, Jeng J. Areca nut extract inhibits the growth, attachment, and matrix protein synthesis of cultured human gingival fibroblasts. *J. Periodontol.* 1998; **69**: 1092–7.

31 Jaffe E, Nachman R, Becker C, Minick C. Culture of human endothelial cells derived from umbilical veins. Identification by morphologic and immunologic criteria. *J. Clin. Invest.* 1973; **52**: 2745–56.

32 Lynch GW, Sloane AJ, Raso V, Cunningham AL. Direct evidence for native CD4 oligomers in lymphoid and monocytoid cells. *Eur. J. Immunol.* 1999; **29**: 2590–602.

33 Lynch GW, Dearden M, Sloane AJ, Humphery-Smith I, Cunningham AL. Analysis of recombinant and native CD4 by one- and two-dimensional gel electrophoresis. *Electrophoresis* 1996; **17**: 227–34.

34 Wright L, Djordjevic J, Schibeci S *et al.* Detergent-resistant membrane fractions contribute to the total 1H NMR-visible lipid signal in cells. *Eur. J. Biochem.* 2003; **270**: 2091–100.

35 Towbin H, Staehelin T, Gordon J. Electrophoretic transfer of proteins from polyacrylamide gels to nitrocellulose sheets: procedure and some applications. *Proc. Natl Acad. Sci. USA* 1979; **76**: 4350–4.

36 Juarez J, Bradstock K, Gottlieb D, Bendall L. Effects of inhibitors of the chemokine receptor CXCR4 on acute lymphoblastic leukemia cells in vitro. *Leukemia* 2003; **17**: 1294–300.

37 Shen W, Bendall LJ, Gottlieb DJ, Bradstock KF. The chemokine receptor CXCR4 enhances integrin-mediated in vitro adhesion and facilitates engraftment of leukemic precursor-B cells in the bone marrow. *Exp. Hematol.* 2001; **29**: 1439–47.

38 Brelot A, Heveker N, Pleskoff O, Sol N, Alizon M. Role of the first and third extracellular domains of CXCR-4 in human immunodeficiency virus coreceptor activity. *J. Virol.* 1997; **71**: 4744–51.

39 Lu Z, Berson JF, Chen Y *et al.* Evolution of HIV-1 coreceptor usage through interactions with distinct CCR5 and CXCR4 domains. *Proc. Natl Acad. Sci. USA* 1997; **94**: 6426–31.

40 Ugolini S, Moulard M, Mondor I *et al.* HIV-1 gp120 induces an association between CD4 and the chemokine receptor CXCR4. *J. Immunol.* 1997; **159**: 3000–8.

41 Lazarini F, Casanova P, Tham TN *et al.* Differential signalling of the chemokine receptor CXCR4 by stromal cell-derived factor 1 and the HIV glycoprotein in rat neurons and astrocytes. *Eur. J. Neurosci.* 2000; **12**: 117–25.

42 Doranz B, Orsini MJ, Turner JD *et al.* Identification of CXCR4 domains that support coreceptor and chemokine receptor functions. *J. Virol.* 1999; **73**: 2752–61.

43 Amara A, Gall S, Schwartz O *et al.* HIV coreceptor down-regulation as antiviral principle: SDF-1alpha-dependent internalization of the chemokine receptor CXCR4 contributes to inhibition of HIV replication. *J. Exp. Med.* 1997; **186**: 139–46.

44 Dimitrov DS, Norwood D, Stantchev TS, Feng Y, Xiao X, Broder CC. A mechanism of resistance to HIV-1 entry: inefficient interactions of CXCR4 with CD4 and gp120 in macrophages. *Virology* 1999; **259**: 1–6.

45 Xiao X, Wu L, Stantchev T *et al.* Constitutive cell surface association between CD4 and CCR5. *Proc. Natl Acad. Sci. USA* 1999; **96**: 7496–501.

46 Vila-Coro AJ, Mellado M, Martin de Ana A *et al.* HIV-1 infection through the CCR5 receptor is blocked by receptor dimerization. *Proc. Natl Acad. Sci. USA* 2000; **97**: 3388–93.

47 Lapham C, Romantseva T, Petricoin E *et al.* CXCR4 heterogeneity in primary cells: possible role of ubiquitination. *J. Leukoc. Biol.* 2002; **72**: 1206–14.

48 Loetscher M, Geiser T, O'Reilly T, Zwahlen R, Baggiolini M, Moser B. Cloning of a human seven-transmembrane domain receptor, LESTR, that is highly expressed in leukocytes. *J. Biol. Chem.* 1994; **269**: 232–7.

49 Berson J, Long D, Doranz B, Rucker J, Jirik F, Doms R. A seven-transmembrane domain receptor involved in fusion and entry of T-cell-tropic human immunodeficiency virus type 1 strains. *J. Virol.* 1996; **70**: 6288–95.

50 Mellado M, Rodriguez-Frade JM, Vila-Coro AJ, de Ana AM, Martinez AC. Chemokine control of HIV-1 infection. *Nature* 1999; **400**: 723–4.

51 Vila-Coro AJ, Rodriguez-Frade JM, Martin De Ana A, Moreno-Ortiz MC, Martinez AC, Mellado M. The chemokine SDF-1alpha triggers CXCR4 receptor dimerization and activates the JAK/STAT pathway. *FASEB J.* 1999; **13**: 1699–710.

52 Sparrow LG, McKern NM, Gorman JJ *et al.* The disulfide bonds in the C-terminal domains of the human insulin receptor ectodomain. *J. Biol. Chem.* 1997; **272**: 29 460–7.

53 Brelot A, Heveker N, Montes M, Alizon M. Identification of residues of CXCR4 critical for human immunodeficiency virus coreceptor and chemokine receptor activities. *J. Biol. Chem.* 2000; **275**: 23 736–44.

54 Potempa S, Picard L, Reeves JD, Wilkinson D, Weiss RA, Talbot SJ. CD4-independent infection by human immunodeficiency virus type 2 strain ROD/B: the role of the N-terminal domain of CXCR-4 in fusion and entry. *J. Virol.* 1997; **71**: 4419–24.

55 Marchese A, Benovic J. Agonist-promoted ubiquitination of the G protein-coupled receptor CXCR4 mediates lysosomal sorting. *J. Biol. Chem.* 2001; **276**: 45 509–12.

56 Manes S, del Real G, Lacalle RA *et al.* Membrane raft microdomains mediate lateral assemblies required for HIV-1 infection. *EMBO Rep.* 2000; **1**: 190–6.

57 Nguyen DH, Hildreth JE. Evidence for budding of human immunodeficiency virus type 1 selectively from glycolipid-enriched membrane lipid rafts. *J. Virol.* 2000; **74**: 3264–72.

58 Ilangumaran S, Arni S, van Echten-Deckert G, Borisch B, Hoessli DC. Microdomain-dependent regulation of Lck and Fyn protein-tyrosine kinases in T lymphocyte plasma membranes. *Mol. Biol. Cell.* 1999; **10**: 891–905.

59 Manes S, Mira E, Gomez-Mouton C *et al.* Membrane raft microdomains mediate front-rear polarity in migrating cells. *EMBO J.* 1999; **18**: 6211–20.

60 Parolini I, Topa S, Sorice M *et al.* Phorbol ester-induced disruption of the CD4–Lck complex occurs within a detergent-resistant microdomain of the plasma membrane. Involvement of the translocation of activated protein kinase C isoforms. *J. Biol. Chem.* 1999; **274**: 14 176–87.

61 Viola A, Schroeder S, Sakakibara Y, Lanzavecchia A. T lymphocyte costimulation mediated by reorganization of membrane microdomains. *Science* 1999; **283**: 680–2.

62 Underhill GH, Kolli KP, Kansas GS. Complexity within the plasma cell compartment of mice deficient in both E- and P-selectin: implications for plasma cell differentiation. *Blood* 2003; **102**: 4076–83.

63 Chabot DJ, Broder CC. Substitutions in a homologous region of extracellular loop 2 of CXCR4 and CCR5 alter coreceptor activities for HIV-1 membrane fusion and virus entry. *J. Biol. Chem.* 2000; **275**: 23 774–82.